

RESEARCH ARTICLE

## Accurate series resistance measurement of solar cells

Kean Chern Fong<sup>1\*</sup>, Keith R. McIntosh<sup>2</sup> and Andrew W. Blakers<sup>1</sup>

<sup>1</sup> Centre for Sustainable Energy Systems, Australian National University, ACT 0200, Australia

<sup>2</sup> PV Lighthouse, 10 Middle Heights Road, Coledale, NSW 2515, Australia

### ABSTRACT

The series resistance ( $R_s$ ) of a solar cell is commonly represented as a constant resistance value. However, because of the distributed nature of series resistance, the effective lumped  $R_s$  vary with current density and illumination intensity. Treating  $R_s$  as a constant is usually insufficient for an accurate analysis of its  $J$ - $V$  curve. This work first presents a review of the distributed nature of series resistance and commonly applied methods to measure  $R_s$ . Particular attention is given to the multi-light method (MLM) and it is discussed in detail, where  $R_s$  in both the light and dark can be measured as a function of current by extracting  $R_s$  from a set of current–voltage ( $J$ - $V$ ) curves attained at different illumination intensities. The principle behind this method is discussed, and the results are then compared with those of other known methods of  $R_s$  measurement. The accurate measurement of  $R_s(J)$  attained with the MLM permits the extraction of an  $R_s$ -corrected  $J$ - $V$  curve, which is theoretically more accurate than that attained by alternative methods because of negligible error from injection dependence and spectral mismatch. With the solar cell equation modified to include  $R_s(J)$ , we attain a much better fit to experimental data, finding a significant reduction in error compared with using a constant  $R_s$ . Copyright © 2011 John Wiley & Sons, Ltd.

### KEYWORDS

series resistance; resistance loss; characterization; solar cell

### \*Correspondence

Fong, Kean Chern, Centre for Sustainable Energy Systems, Australian National University, ACT 0200, Australia.

E-mail: kean.fong@anu.edu.au

Received 13 April 2011; Revised 25 July 2011; Accepted 5 September 2011

## 1. INTRODUCTION

One of the loss mechanisms limiting the performance of a solar cell is the ohmic series resistance loss ( $R_s$ ), which arises from the resistance within the device itself. It is a parasitic effect that cannot be eliminated but can be reduced by better design. The effective resistance in a device is often represented by a constant lumped  $R_s$ . Because of its simplicity, the constant lumped  $R_s$  is widely applied in the analysis of solar cells. However, assuming that the  $R_s$  as a constant value is an oversimplification. The distributed nature of  $R_s$  has been studied extensively over many decades with  $R_s$  divided into many different components such as resistance in the emitter, substrate, metal contacts and metal connections on the device [1,2]. Analysis of  $R_s$  by taking into consideration the voltage drop across the emitter and base in the given geometry of the device was performed, and it was found that the voltage across the emitter in conventional solar cells is the main factor in distributed nature of series resistance [3–5].

Analyses that demonstrate the change in  $R_s$  at different voltage and current in different illumination intensities have been presented by Smirnov and Mahan and later by

Araujo, Cuevas and Ruiz [6,7]. These analyses show that the distributed series resistance causes the measurable effective  $R_s$  to vary with voltage and current. The results by Araujo indicated that the effective  $R_s$  in an illuminated solar cell is higher at low voltages and reaches a minimum at open-circuit voltage, with a theoretical upper and lower bound defined by the bulk and emitter resistivity.

In order to visually illustrate the effects of distributed nature of  $R_s$ , simulation of the examined cell structure was performed using Sentaurus simulation package (Synopsys, Mountain View, CA, USA). Figure 1 shows the changing current flow pattern from the cross section of an elongate solar cell (p-type bulk, contacts on the sidewalls, n+ emitters along front and rear surfaces). Because the voltage drop caused by series resistance is affected by the path and magnitude of current flow, the  $R_s$  at each bias point is different. It is therefore not surprising that even at a fixed illumination intensity, the effective  $R_s$  can still be a function of voltage and current [8,9].

Similar and more in-depth investigations using computer simulations provided interpretation of distributed resistance of other silicon solar cell designs such as the passivated emitter rear locally diffused cell (PERL) and

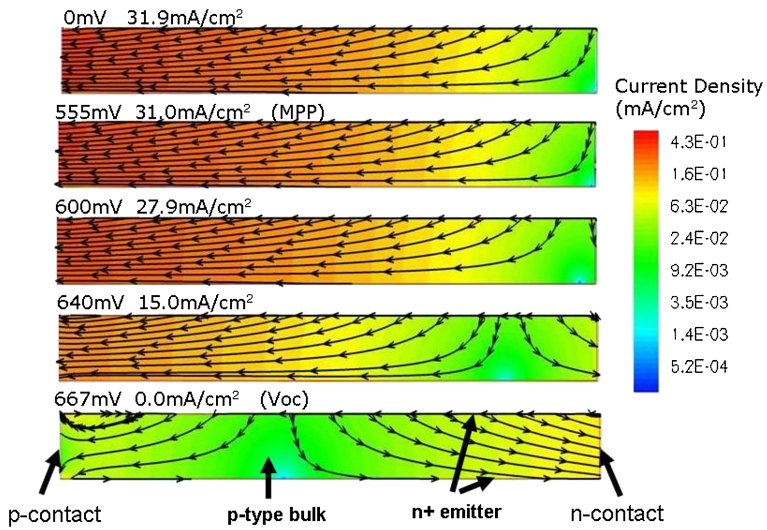


**Figure 1.** Current density and current flow of elongate solar cell (cross section) under 1 sun illumination captured at various voltages.

emitter wrap through cells [8,10,11]. Such analysis of series resistance enabled comprehensive loss analysis of high-efficiency solar cells [11,12].

Several studies performed to compare results between methods of  $R_s$  measurement show that there is significant discrepancy between well-known methods [13,14]. The main reason such discrepancies are observed is because each measurement method is performed at a different light intensity or current level [9,15–18].

There are two published works that accurately measure  $R_s$  as a function of current (or voltage). The first is a method proposed by Aberle *et al.* [10], which obtains  $R_s$  by comparing the  $J_{sc}$ – $V_{oc}$  curve with the illuminated  $J$ – $V$  curve (shifted to the first quadrant). The difference in voltage between the two  $J$ – $V$  curves at each current point is the voltage drop across the lumped series resistance, and therefore each current point on the  $J$ – $V$  curve can be analysed to attain  $R_s(J)$ . The double-light method (DLM) [1,8,19] attains  $R_s(J)$  by measuring  $R_s$  at different voltage points on the  $J$ – $V$  curve. Both methods do correlate well and have shown very good agreement with 2D simulation of the PERL solar cell. However, there is a limitation to each method. Because the  $J_{sc}$ – $V_{oc}$  curve is constructed by measurements from a huge range of illumination intensity, the injection level within the device changes by several orders of magnitude across the range of measurement. In ideal cases (such as in solar cell models), the saturation current  $J_o$  terms are constants. However, these are never true in actual devices because recombination terms (which defines the saturation current) varies with injection level and applied voltage, causing inaccuracies in the  $R_s$  measurement. The problem of illumination intensity is much more manageable for the DLM, where the illumination intensity between the two  $J$ – $V$  curves can be kept small (<10%). However, whenever the change in illumination intensity is too small, the measurable voltage shift for DLM is also very small, and the measurement becomes sensitive to equipment error or noise level in the light.

This paper clarifies several points regarding different  $R_s$  measurement methods and presents the multiple-light method (MLM), which can accurately extract  $R_s$  as a function of current  $R_s(J)$  over a large voltage range. It is an extension of the DLM and improves upon it by using multiple  $J$ – $V$  curves, measuring  $R_s$  across the entire current range at very small increments of  $\Delta J$ . By performing  $J$ – $V$  curves at multiple illumination intensities (three or more), it is possible to attain better measurement accuracy at low voltages.

As will be demonstrated, an  $R_s$ -corrected  $J$ – $V$  curve allows extraction of pseudo-efficiency and  $R_s$ -corrected local ideality factor and allows more accurate parameterization. The principle behind the method is discussed, and the condition to provide accurate measurement is investigated.

## 2. PRINCIPLE OF MEASUREMENT

### 2.1. Experimental setup

The experimental setup used for the work presented in this work utilises a halogen lamp with a current controlled power supply. The temperature of the device under test is controlled with a Peltier cooled heat sink attached to a thermocouple feedback loop temperature controller. The thermocouple is attached to an adjacent identical cell rather than on the heat sink for better temperature control. The measurements and voltage load were performed using a Keithley 2400 source meter (Keithley Instruments Inc., Cleveland, Ohio). The raw measurement data is then sent to an interfaced computer, which logs the measurements and performs the  $R_s(J)$  calculations. Because of the spectral variation in the light at different power levels, a set of grey filters was used to control the illumination intensity so that only small current adjustments were necessary to achieve desired intensity.

## 2.2. Measurement principle of $R_s$ using double illumination method

The principle behind measuring  $R_s(J)$  is an extension of the double illumination method, which was originally published by Wolf and Rauschenbach [1]. In order to fully understand the principle and, more importantly, the assumptions contained in this method, it is derived here from the single-exponential model of a solar cell:

$$J = J_o \left[ \exp\left(\frac{V + JR_s}{mV_{th}}\right) - 1 \right] - J_L \quad (1)$$

where  $V_{th} = \frac{q}{kT}$  and  $m$  is the local ideality factor,  $q$  is the electron charge,  $k$  is Boltzmann's constant and  $T$  is the absolute temperature.

When the difference in the illumination intensity between the measurements is sufficiently small that it does not alter the current paths and operating conditions of the cell, we can also assume that  $m$ ,  $J_o$  and  $R_s$  are constant. These assumptions are not always true and will be discussed further in Section 5. Solving Equation 1 for two different illumination intensities by equating  $J_o$  and taking the logarithms, we obtain Equation 2.

$$\ln\left(\frac{J^{(1)} + J_L^{(1)}}{J^{(2)} + J_L^{(2)}}\right) = \left(\frac{V^{(1)} + J^{(1)}R_s}{mV_{th}} - 1\right) - \left(\frac{V^{(2)} + J^{(2)}R_s}{mV_{th}} - 1\right) \quad (2)$$

The superscripted numbers in brackets denote values from the first  $J-V$  curve and the second  $J-V$  curve. By keeping temperature constant over every  $J-V$  curve, we can assume  $V_{th}^{(1)} = V_{th}^{(2)}$ . Because  $J^{(1)}$  is a negative term,  $J^{(1)} + J_L^{(1)}$  is the current difference,  $\Delta J$ , shown in Figure 2. By selecting the same  $\Delta J$  for both the first and second  $J-V$  curve,  $J^{(1)} + J_L^{(1)} = J^{(2)} + J_L^{(2)}$ , and so the left side of Equation 2 is null. The equation is then solved for  $R_s$ .

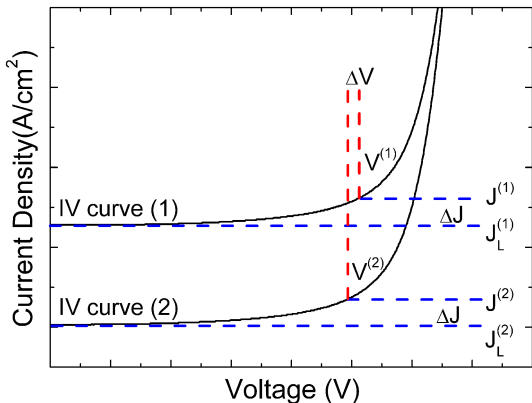


Figure 2. Illustration of double illumination method.

$$R_s = \frac{V^{(1)} - V^{(2)}}{J^{(2)} - J^{(1)}} = \frac{1}{\text{slope of line}} \quad (3)$$

Thus,  $R_s$  is the inverse of the slope of the line joining the  $J-V$  points 1 and 2.

## 2.3. Multi-light method to determine $R_s(J)$

The same principle can be applied to three or more  $J-V$  curves, where a central  $J-V$  curve at 1-sun intensity is measured, and any number of  $J-V$  curves can be measured with increasing and decreasing illumination intensity relative to the central  $J-V$  curve. For  $n$  number of  $J-V$  curves,  $R_s$  on the (central)  $J-V$  curve is

$$R_s(J) = \frac{\left| \begin{array}{c} \sum_{i=1}^{i=n} (V_i - \bar{V})^2 \\ \sum_{i=1}^{i=n} (V_i - \bar{V})(J_i - \bar{J}) \end{array} \right|}{\left| \begin{array}{c} \sum_{i=1}^{i=n} (V_i - \bar{V}) \\ \sum_{i=1}^{i=n} (V_i - \bar{V})(J_i - \bar{J}) \end{array} \right|} \quad (4)$$

By performing the same  $R_s$  measurement at small increments of  $\Delta J$ ,  $R_s$  as a function of current  $R_s(J)$  is extracted. The application of this method is illustrated in Figure 3, where measurements are taken at four points with incrementing  $\Delta J$ . This method can be implemented for flash type  $I-V$  testers where multiple illumination intensities are measured simultaneously. Both DLM and MLM measure the differential  $R_s$  and not the absolute value. However, it can be shown that the difference between differential and actual  $R_s$  values is small [20,21].

## 3. MEASUREMENT RESULTS

Figures 4 and 5 present the results of MLM (using three  $J-V$  curves) measurement for a commercial interdigitated back contact solar cell and elongate solar cells fabricated at Australian National University with high, moderate and low emitter sheet resistivity, labelled as EL-HiEmiT, EL-MedEmiT and EL-LowEmiT, respectively. By looking at

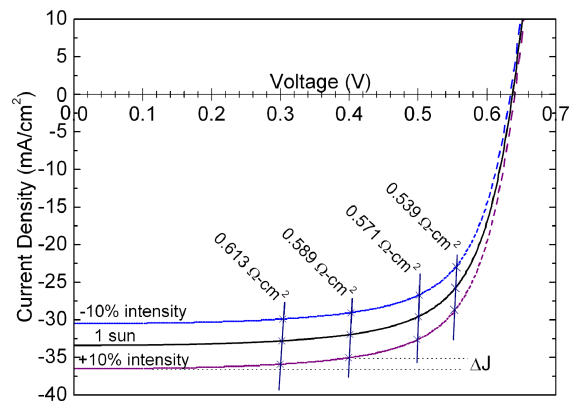
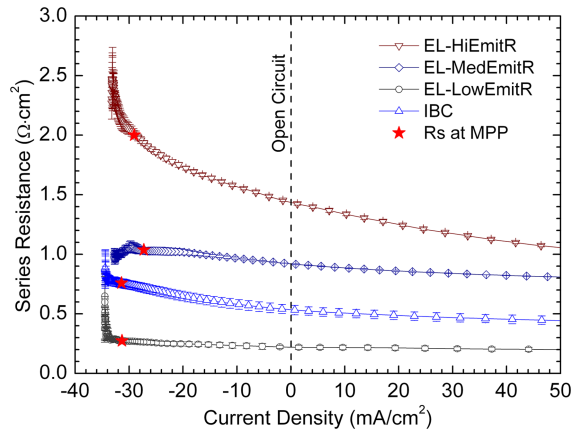
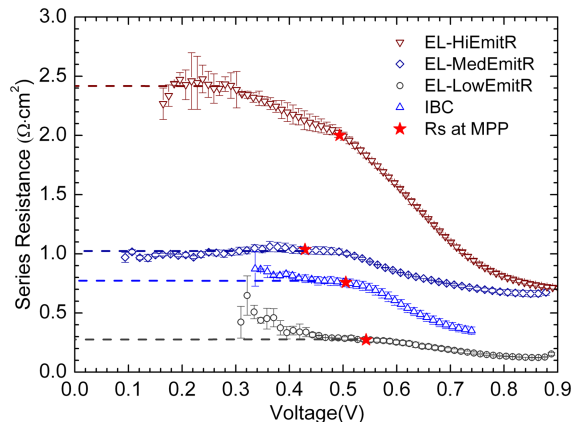


Figure 3. Series resistance measurement is taken at four points along the  $J-V$  curve at increasing  $\Delta J$ .



**Figure 4.** Series resistance plotted against current density,  $R_s(J)$  for elongate solar cells of different emitter resistivity and a commercially available interdigitated back contact (IBC) solar cell.



**Figure 5.** Series resistance plotted against voltage for elongate solar cells of different emitter resistivity and a commercially available interdigitated back contact (IBC) solar cell. Data points at low voltages were removed because of excessively high error range.

$R_s$  as a function of voltage (Figure 5), the characteristic  $R_s(V)$  curve as demonstrated in the modelling by Araujo *et al.* [7] is observed. In some cases, the  $R_s$  at low voltage cannot be accurately measured because of limitations in the stability of the light source. However, as is shown in Figure 1, the current density and current flow within the device do not change significantly at low voltages, and therefore the effective  $R_s$  at low  $V$  should remain constant.

A comparison between DLM and MLM was performed for 10 sets of  $J-V$  curves. DLM was calculated using  $I-V$  curves at 110% and 90% of the 1-sun illumination intensity. MLM-3  $I-V$  curves utilised the same data as the DLM measurement with the addition of an  $I-V$  curve at 100%. MLM-5  $I-V$  curves utilised the same data as the MLM-3 curves with the addition of  $I-V$  curves at 107% and 93%. MLM-7  $I-V$  curves utilised the same data as the MLM-5 curves with the addition of  $I-V$  curves at 108.5% and 91.5%. The plotted results in Figure 6 are

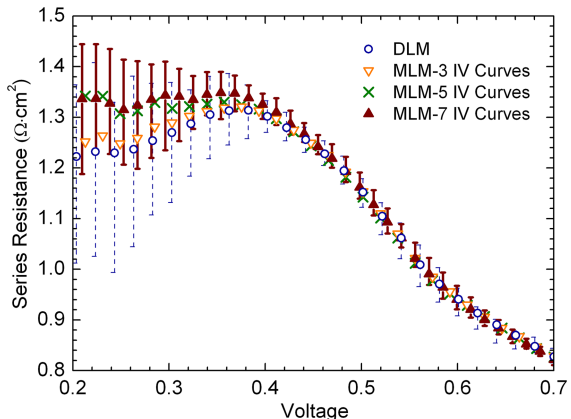


**Figure 6.** Comparison of measurement and standard deviation between double-light method (DLM) and multi-light method (MLM) (3, 5 and 7 light intensities). Only error bars for DLM and MLM-7 IV curves are plotted, representing the measured maximum and minimum values.

the average of the 10 measurements, and the error bars for DLM and MLM-7 are the minimum and maximum calculated values off  $R_s$ . The difference between DLM and MLM is the better consistency with more number of  $J-V$  curves, with MLM results correctly showing the constant  $R_s$  value at low voltages. There is no significant difference between the results at voltages above the maximum power point (MPP).

### 3.1. Extracting the $R_s$ -corrected $J-V$ curve

The  $J-V$  curve of a solar cell can provide much information about the performance and loss mechanisms of the cell. However, the series resistance often dominates at the high-voltage region of the  $J-V$  characteristics, which affects accurate analysis of the p-n junction of the cell. There are two published methods to obtain the  $R_s$ -corrected  $J-V$  curve, which are the Suns- $V_{oc}$  method and the  $J_{sc}-V_{oc}$  method [10,22]. Both methods measure the  $J-V$  curve by combining  $V_{oc}$  points across a large range of illumination intensity. As discussed in Section 1, the dependence of saturation currents on injection level will cause inaccuracy in such measurements.

By using the MLM method,  $R_s(J)$  is measured using  $J-V$  curves of similar illumination intensity (10% difference), and there is no significant difference in carrier injection, and thus there is small error from such effects. Utilising grey filters to control the illumination intensity also minimises error from spectral mismatch. Therefore,  $R_s(J)$  can be used to offset the main  $J-V$  curve to provide an  $R_s$ -corrected  $J-V$  curve with little error from injection-dependent effects and spectral mismatch.

When the cell is illuminated, current is drawn from the cell, and the voltage measured through the terminals,  $V_m$ , is the voltage across the p-n junction minus the voltage lost to series resistance,  $V_{Rs}$ . Because  $V_{Rs}=J \times R(J)$ , we can

calculate the  $R_s$ -corrected voltage,  $V_{Rs\text{-corrected}}$ , by offsetting the measured voltage with the voltage lost to resistive effects:

$$V_{Rs\text{-corrected}}(J) = V_m(J) + J_m R_s(J) \quad (5)$$

Because  $R_s$  at each voltage point on the  $J$ - $V$  curve is known, the correction for the entire  $J$ - $V$  curve can be performed. The obtained  $R_s$ -corrected  $J$ - $V$  curve for cell EL-HiEmitR is plotted in Figure 7(a) and shows very good agreement with the  $J_{sc}$ - $V_{oc}$  curve even beyond open-circuit voltage.

### 3.2. Determination of $J_L$

The solar cell equation can be rewritten as a function of  $J_L$  where  $V=0$  and  $J=J_{sc}$ . Because  $R_s$  at  $V=0$  is a difficult value to measure, we will assume that  $R_s$  does not vary

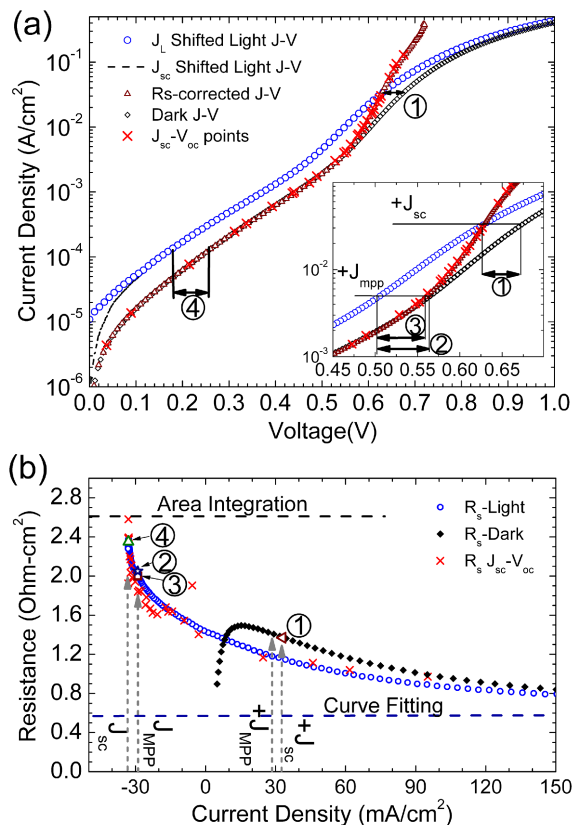


**Figure 7.** (a)  $J$ - $V$  curve of cell EL-HiEmitR showing the light  $J$ - $V$  curve (shifted by  $J_L$  and  $J_{sc}$ ), dark  $J$ - $V$  curve and  $R_s$ -corrected  $J$ - $V$  curve plotted with measurement points for other  $R_s$  measurement methods. (b) Results of  $R_s(J)$  measurement from multi-light method,  $J_{sc}$ - $V_{oc}$ , area integration method, curve fitting and other methods (numbered). Numbered points represent  $R_s$  measurements by  $\Delta V/J$  where  $\Delta V$  is (1)  $V_{dark}-V_{light}$  at  $J_{sc}$ , (2)  $V_{dark}-V_{light}$  at maximum power point (MPP), (3)  $V_{light}-V_{Rs\text{-corrected}}$  at MPP and (4)  $V_{dark}-V_{light}$  at low voltage.

significantly at low voltages [7] and the maximum  $R_s$  measured is used (dashed lines in Figure 5). All other parameters in Equation 6 can be obtained by iteratively fitting the solar cell equation to the light  $J$ - $V$  curve. At  $V=0$ , the  $J_{o1}$  term is negligibly small, and only significant terms are the  $J_{o2}$  term and the shunt resistance term. For the case of elongate solar cells, an additional recombination term due to an exposed unpassivated p-n junction region (arising from separation of the cell from its host wafer) is taken into account in the calculation of  $J_L$  (details of elongate cell modelling is presented in Section 4).

$$J_L = J_{sc} + J_{o1} \left[ \exp\left(\frac{J_{sc} R_s(V=0)}{V_{th}}\right) - 1 \right] + J_{o2} \left[ \exp\left(\frac{J_{sc} R_s(V=0)}{2V_{th}}\right) - 1 \right] + \frac{J_{sc} R_s(V=0)}{R_{shunt}} \quad (6)$$

The practice of shifting the light  $J$ - $V$  curve by  $J_{sc}$  into the first quadrant causes the dark  $J$ - $V$  and light  $J$ - $V$  to converge at  $V=0$ , which is not an accurate representation of the shifted light  $J$ - $V$  curve because it implies that  $R_s=0$  at  $V=0$  (which is impossible). The difference between  $J_L$  and  $J_{sc}$  for cells in this work is in the order of  $1 \times 10^{-5}$  mA/cm<sup>2</sup>. Figure 7(a) illustrates the difference between shifting by  $J_{sc}$  and  $J_L$ . This provides a more accurate representation of the  $R_s$ -corrected  $J$ - $V$  curve where  $R_s$  does not approach zero at 0 V.

### 3.3. Extracting $R_{s\text{-dark}}$ from $R_s$ -corrected $J$ - $V$ curve

In the dark, the voltage bias is applied through the solar cell from an external source, and current is injected through the device via the lowest resistive path. This cause the current to flow in a different pattern across the device (metallization and within the cell), thus causing a difference between  $R_{s\text{-dark}}$  and  $R_{s\text{-light}}$ . Other illumination-dependent factors that will affect the resistivity between light and dark condition is the change in the behaviour of the p-n junction under illumination and also the conductivity of the semiconductor when illuminated.

In the dark condition, the voltage source is external, and so the measurable voltage drop across the solar cell terminals is the voltage across the p-n junction,  $V_{Rs\text{-corrected}}$ , and the voltage caused by series resistance,  $R_{s\text{-dark}}$ .  $R_{s\text{-dark}}$  can be measured from the voltage shift between the known  $R_s$ -corrected  $J$ - $V$  curve and the dark  $J$ - $V$  curve as represented in Equation 7.

$$R_{s\text{-dark}}(J_m) = \frac{V_{dark} - V_{Rs\text{-corrected}}}{J_m} \quad (7)$$

Figure 7(b) shows the extracted  $R_{s\text{-dark}}$ . Although  $R_{s\text{-dark}}$  can be extracted from an  $R_s$ -corrected  $J$ - $V$  curve taken at 1 sun, there can be a large injection level difference at lower voltages. Thus, to avoid the change in material property due to strong illumination,  $R_s$ -correction of the  $J$ - $V$

curve can be performed at very low illumination intensities. For instance, MLM can be performed with a main illumination intensity of 1/20 sun to measure the  $R_s$ -corrected  $J$ - $V$  curve, which is then used for the extraction of  $R_{s\text{-dark}}$ .

### 3.4. Comparison with other $R_s$ methods

This section compares  $R_s(J)$  and the  $R_s$ -corrected  $J$ - $V$  curve to the  $J_{sc}$ - $V_{oc}$  method and several other  $R_s$  measurement methods that are based on comparison between the light and dark  $J$ - $V$  curves.

#### 3.4.1. Comparison with $R_s$ from $J_{sc}$ - $V_{oc}$

$R_s$  can be extracted by comparing the voltage shift between the  $J_{sc}$ - $V_{oc}$  curve and the lighted  $J$ - $V$  curve. As with the MLM method,  $R_s$  can be measured as a function of current density by measuring at different points.  $R_s(J)$  for  $J_{sc}$ - $V_{oc}$  is calculated as follows:

$$R_s(J_m) = \frac{V_{J_{sc}-V_{oc}} - V_{light}}{J_m} \quad (8)$$

Figure 7 shows the measured  $J_{sc}$ - $V_{oc}$  curve and the extracted  $R_s(J)$  value. The same light source for the MLM method was used with the illumination set to 1-sun intensity and varied using a series of grey filters.  $J_{sc}$ - $V_{oc}$  points at higher illumination intensity were achieved by moving the light source closer to the cell. The  $R_s(J)$  value extracted from the  $J_{sc}$ - $V_{oc}$  method shows good correlation below and beyond open-circuit current.

Near  $V_{oc}$  point, all three measured values ( $V_{J_{sc}-V_{oc}}$ ,  $V_{light}$  and  $J_m$ ) are very small, making the measurement very sensitive to error in voltage measurement. To obtain accurate  $R_s$  value near  $V_{oc}$  using the  $J_{sc}$ - $V_{oc}$  method, the authors have found that temperature must be controlled meticulously and identical light source must be used for both the  $J_{sc}$ - $V_{oc}$  and the 1 sun light  $J$ - $V$  measurement.

#### 3.4.2. Comparison with $R_s$ from light versus dark $J$ - $V$ curve analysis

Both the dark and light  $J$ - $V$  curves are easily measured, and therefore methods to measure  $R_s$  from the comparison of dark and light are convenient. Performing light versus dark  $J$ - $V$  measurement of  $R_s$  [10] takes the  $\Delta V$  between the shifted light  $J$ - $V$  curve and the dark  $J$ - $V$  curve divided by the current. Because of the opposing current flow direction between dark and lighted condition, the measured voltage across the solar cell terminals differ between the light and dark conditions (Equations 9 and 10).

$$V_{light} = V_{diode} - J_{light} \times R_{s\text{-light}} \quad (9)$$

$$V_{dark} = V_{diode} + J_{dark} \times R_{s\text{-dark}} \quad (10)$$

The voltage difference between the dark and light  $J$ - $V$  is defined as

$$\Delta V = V_{dark} - V_{light} = J_{dark}R_{s\text{-dark}} + J_{light}R_{s\text{-light}} \quad (11)$$

As we can see from the definition of  $\Delta V$ , either one of  $R_s$  can be solved only if either  $J_{light}$  or  $J_{dark}$  is null or extremely small. By choosing  $\Delta V$  at a current magnitude equivalent to  $J_{sc}$  (point 1 in Figure 7), where  $J_{light}=0$ ,  $R_{s\text{-dark}}$  can be solved as

$$R_{s\text{-dark}} = \frac{\Delta V}{J_{sc}} \quad (12)$$

However, it must be noted that  $R_{s\text{-dark}}$  equals to  $R_{s\text{-light}}$  only in the ideal 1D condition and is not necessarily true for actual solar cells.

$R_{s\text{-light}}$  at MPP can be solved by assuming  $J_{dark}$  to be negligible at MPP [10]. The implementation of this method is shown in point 2 of Figure 7 where Equation 11 is solved for  $R_{s\text{-light}}$ :

$$R_{s\text{-light}} \cong \frac{\Delta V}{J_{light\text{-mpp}}} \quad (13)$$

In the case of this device, the actual voltage shift caused by  $R_{s\text{-light}}$  at MPP is smaller, as illustrated at point 3 of Figure 7. Applying the voltage measured at point 2 will cause  $R_s$  to be slightly overestimated. Therefore, this technique must be applied with caution because the assumption that  $J_{dark}$  is negligible at MPP is not always true for all solar cells.

On the other hand, this assumption is much safer to make at lower voltages where  $J_{dark}$  is several orders of magnitude smaller than  $J_{light}$ . For example, the  $J_{dark}$  at point 4 in Figure 7(a) is two orders of magnitude smaller compared to  $J_{light}$  (non-shifted), thus making the effect of series resistance on the dark  $J$ - $V$  curve negligible.

The results for each of the measurement methods discussed are illustrated in Figure 7(b).

#### 3.4.3. Comparison to $R_s$ from single light $J$ - $V$ curve

Two other methods, area integration [9] and curve fitting [23], are also plotted in Figure 7(b) (the curve fitting was performed by fitting the light  $J$ - $V$  curve to the dual exponential model using orthogonal distance regression). These methods do not measure  $R_s$  as a function of current, so a fixed  $R_s$  value is plotted. Once again there is a large discrepancy between these values and  $R_s$  values from other methods. This is mainly because cell EL-HiEmitR has very highly distributed  $R_s$ . This is not necessarily the case for all solar cells. For instance,  $R_s$  values from various methods will have significantly better agreement for the EL-Low EmitR and interdigitated back contact cell shown in Figures 4 and 5.

#### 4. PARAMETERIZATION USING $R_s$ ( $J$ ) AND ANALYSIS OF $R_s$ -CORRECTED J-V CURVE

Solar cells with current-dependent  $R_s$  cannot be described accurately using the standard single or double exponential models (which assume a constant  $R_s$ ). The  $R_s(J)$  of cell EL-HiEmitR is a good example of such a device. In order to fit the  $J$ - $V$  curve of the elongate cells, Equation 14, which is an extended version of the double exponential model with a resistance limited high recombination centre, is applied [24]. The fixed  $R_s$  terms are also replaced with  $R_s(J)$ . (The terms  $J_{o1}$  and  $J_{o2}$  are the standard saturation current terms for the two diodes of local ideality factor 1 and 2, respectively. The  $J_{oH}$  term is a cell design specific

recombination term found to be related to unpassivated p-n junction regions because of the removal of a cell from the host wafer. The reason  $J_{oH}$  term has a factor of two is due to having two such identical surfaces in the elongate cells at each end.)

$$J = J_L - J_{o1} \left[ \exp\left(\frac{V + JR_s(J)}{V_{th}}\right) - 1 \right] - J_{o2} \left[ \exp\left(\frac{V + JR_s(J)}{2V_{th}}\right) - 1 \right] - 2J_{oH} \left[ \exp\left(\frac{V + JR_s(J) - V_H R_H}{2V_{th}}\right) - 1 \right] - \frac{V + JR_s(J)}{R_{shunt}} \quad (14)$$

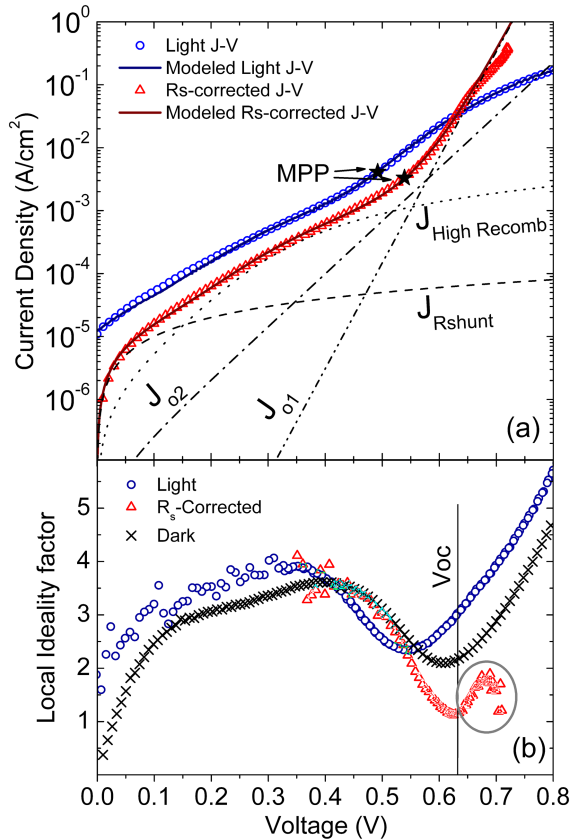


**Figure 8.** (a)  $R_s$ -corrected  $J$ - $V$  curve of cell EL-HiEmitR compared with modelled curves and (b) local ideality factor of light, dark and  $R_s$ -corrected  $J$ - $V$  curve.

By using the measured  $R_s(J)$ , the model provides a very good fit to experimental  $J$ - $V$  curve (Figure 8(a)). In contrast, when a similar model with the  $R_s$  fixed at  $R_s$ -MPP is used, a good fit cannot be achieved especially for the high-voltage region where  $R_s$  is significantly overestimated. There is also a significant difference in the extracted parameters from the curve fitting. Table I summarises the results of curve fitting using  $R_s(J)$  model versus using a fixed  $R_s$  on the same lighted  $J$ - $V$  data. This shows that modelling with a fixed  $R_s$  value can lead to erroneous evaluations, and a model with  $R_s(J)$  should be used when there is significant distributed resistance effects.

The pseudo-parameters can also be extracted directly from the  $R_s$ -corrected  $J$ - $V$  curve. Table II shows the comparison between the experimental result and the  $R_s$ -corrected  $J$ - $V$  curve. The extracted data from the  $R_s$ -corrected  $J$ - $V$  curve gives an indication of the performance of the device without  $R_s$  losses. The MMPs are also plotted in Figure 8(a).

Figure 8(b) plots the  $R_s$ -corrected local ideality factor along with the dark and light local ideality factor. The light and dark measurements becomes dominated by the series resistance effects beyond 0.5 V, but the  $R_s$ -corrected local ideality factor clearly shows local ideality factor of the device without  $R_s$  effects beyond 0.5 V. The resulting measurement on cell EL-HiEmitR exposed an underlying recombination effect, which attributed itself as a bump with a peak at 680 mV. This bump is consistent with the case when  $\sigma_p \ll \sigma_n$  for p-type solar cells, which can be caused by numerous effects such as oxide charges and defects at the surface [25], boron-induced dislocations [26] or presence of metal impurities [27].

**Table I.** Results of curve fitting and parameterization of cell EL-HiEmitR using the  $R_s(J)$  model and a fixed  $R_s$  model.

Method	$J_{o1}$ (A/cm <sup>2</sup> )	$J_{o2}$ (A/cm <sup>2</sup> )	$R_{sh}$ ( $\Omega$ cm <sup>2</sup> )	$2J_{oH}$ (A/cm <sup>2</sup> )	$R_H$ ( $\Omega$ cm <sup>2</sup> )	Chi-square of fit
Modelled with $R_s(J)$	$4.9 \times 10^{-13}$	$4.1 \times 10^{-8}$	8000	$5.99 \times 10^{-7}$	126	0.0053
Fixed $R_s$ ( $R_s$ MPP 2.05 $\Omega$ cm <sup>2</sup> )	$4.0 \times 10^{-13}$	$3.5 \times 10^{-8}$	7200	$7.8 \times 10^{-7}$	114	8.7129
% Difference	-18.37	-15.38	-10	+30.26	-9.52	—

MPP, maximum power point.

**Table II.** Results of analysis from  $R_s$ -corrected  $J$ – $V$  curve of cell EL-HiEmitR.

Parameter	Full circuit	$R_s$ -corrected
$R_s$ at MPP ( $\Omega \text{ cm}^2$ )	2.05	0
$V_{\text{MPP}}$ (mV)	492	539
$J_{\text{MPP}}$ ( $\text{mA/cm}^2$ )	29.0	29.8
$FF$	0.69	0.77
Efficiency (%)	14.31	16.07

MPP, maximum power point.

**Table III.** Setup of temperature sensitivity test.

Measurement	Temperature ( $^{\circ}\text{C}$ )		
	Main $J$ – $V$ curve	High-intensity $J$ – $V$ curve	Low-intensity $J$ – $V$ curve
25 $\pm 0.1^{\circ}\text{C}$	25	25	25
25 $\pm 0.3^{\circ}\text{C}$	25	25.3	24.7
25 $\pm 0.6^{\circ}\text{C}$	25	25.6	24.4
25 $\pm 0.9^{\circ}\text{C}$	25	25.9	24.1
25 $\pm 1.2^{\circ}\text{C}$	25	26.2	23.8
25 $\pm 1.5^{\circ}\text{C}$	25	26.5	23.5

## 5. MEASUREMENT SETUP CONSIDERATIONS

In order to obtain accurate measurement with this technique, the assumptions made in Section 2.2 must be taken into account during the design of the measurement. All of the parameters  $m$ ,  $I_o$ ,  $R_s$  and  $V_{\text{th}}$  are assumed to be equal between different  $J$ – $V$  measurements but are actually affected by the voltage, the current, the light intensity and the temperature. Because the illumination intensity must be varied between different  $J$ – $V$  measurements, none of these assumptions are completely true.

Difference between the  $m$ ,  $I_o$  and  $R_s$  can be kept small by choosing a smaller difference in illumination intensity. The results in this work use a 10–15% difference between illumination intensity. Generally, the larger the illumination intensity difference, the more consistent the results (due to reduced relative measurement uncertainty), but the more error is introduced from the assumption of constant values of  $m$ ,  $I_o$  and  $R_s$ . Illumination intensity difference below 15% was found to provide very good correlation with  $J_{\text{sc}}\text{--}V_{\text{oc}}$  results.

The value of  $V_{\text{th}}$  is kept constant by ensuring that the temperature does not change between illumination intensities. When the temperature is not constant, the measured  $R_s$  value starts to deviate from the controlled measurement results. This error is expected because it can be seen from Equation 1 that the temperature of the cell directly affects the voltage. To demonstrate the importance of accurate temperature control, a series of measurements were taken with small temperature changes between each  $J$ – $V$  curves. The details of the experimental setup are documented in Table III.

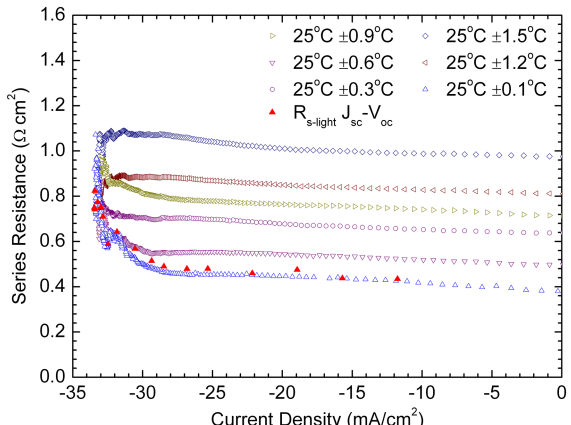
**Figure 9.**  $R_s(J)$  measurement with deliberately introduced error in temperature.

Figure 9 shows that small temperature changes between  $J$ – $V$  curves significantly affect the measurement and the temperature must be controlled to within  $\pm 0.1^{\circ}\text{C}$  in order to obtain an accurate measurement.

For all experiments performed, the thermocouple was attached to the top surface of an identical dummy cell. Although some error may be caused from temperature gradient between the top surface and the bottom surface of the device, this was not investigated as part of this work. Cells used in this work are relatively thin, between 80 and 150  $\mu\text{m}$ .

## 6. CONCLUSION

Because of the distributed nature of series resistance in solar cells, the measurable effective series resistance varies with the operating conditions. In general, both  $R_{s\text{-light}}$  and  $R_{s\text{-dark}}$  are higher at lower voltages and reduce as the voltage across the terminal is increased. In devices with significant distributed  $R_s$ , the effective  $R_s$  can vary significantly between  $V_{\text{oc}}$  and  $V_{\text{MPP}}$ , and therefore a single value of  $R_s$  cannot adequately describe the device. An accurate representation of resistance in such devices must be a function of current (or voltage).

Several methods of  $R_s(J)$  measurements were discussed, and the MLM was shown to provide the most accurate  $R_s$  measurement, with more  $J$ – $V$  curves providing better consistency and accuracy. The MLM does not assume a particular model or value of local ideality factor and therefore is applicable for any silicon solar cell design. It provides better accuracy because the measurement is performed at similar illumination intensity to actual operating conditions, and thus there is minimal error from variation due to dependence on injection levels. Therefore, the calculated  $R_s$ -corrected  $J$ – $V$  curve from the MLM is a more accurate representation of the resistance-free lighted  $J$ – $V$  curve. The need to measure multiple  $J$ – $V$  curves is not necessarily

more difficult as it can be easily implemented in flash type *I*-*V* testers where multiple illumination intensities are measured simultaneously.

Modelling of solar cells with highly variable  $R_s$  was demonstrated with the incorporation of  $R_s(J)$  into the solar cell equation. Curve fitting of the model to cell EL-HiEmitR achieved a better fit when compared with using a constant  $R_s$  ( $R_s$  at MPP). The fixed  $R_s$  model had a significant degree of error in parameterization of the device, with as much as 10% to 30% variation when compared with parameters attained using the  $R_s(J)$  model.

## ACKNOWLEDGEMENTS

Thanks to Prof. Andres Cuevas who has graciously shared his experience in the discussions we had on  $R_s$  measurement methods.

## REFERENCES

- Wolf M and Rauschenbach H. Series resistance effects on solar cell measurements. *Advanced Energy Conversion* 1963; **3**: 455–479.
- Handy RJ. Theoretical analysis of the series resistance of a solar cell. *Solid-State Electronics* 1967; **10**: 765–775.
- Wyeth NC. Sheet resistance component of series resistance in a solar cell as a function of grid geometry. *Solid-State Electronics* 1977; **20**: 629–634.
- Boone JL and van Doren TP. Solar-cell design based on a distributed diode analysis. *Electron devices. IEEE Transactions on* 1978; **25**: 767–771.
- Nielsen LD. Distributed series resistance effects in solar cells. *Electron devices. IEEE Transactions on* 1982; **29**: 821–827.
- Smirnov GM and Mahan JE. Distributed series resistance in photovoltaic devices; intensity and loading effects. *Solid-State Electronics* 1980; **23**: 1055–1058.
- Araujo GL, Cuevas A and Ruiz JM. The effect of distributed series resistance on the dark and illuminated current-voltage characteristics of solar cells. *Electron devices. IEEE Transactions on* 1986; **33**: 391–401.
- Altermatt PP, Heiser G, Aberle AG, et al. Spatially resolved analysis and minimization of resistive losses in high-efficiency Si solar cells. *Progress in Photovoltaics: Research and Applications* 1996; **4**: 399–414.
- Araujo GL and Sanchez E. A new method for experimental determination of the series resistance of a solar cell. *Electron devices IEEE Transactions on* 1982; **29**: 1511–1513.
- Aberle AG, Wenham SR and Green MA. A new method for accurate measurements of the lumped series resistance of solar cells. *Photovoltaic Specialists Conference, Louisville*, 1993; 133–139.
- Ulzhofer C, Altermatt PP, Harder N and Brendel R. Loss analysis of emitter-wrap-through silicon solar cells by means of experiment and three-dimensional device modeling. *Journal of Applied Physics* 2010; **107**: 104509.
- Aberle AG, Altermatt PP, Heiser G, et al. Limiting loss mechanisms in 23% efficient silicon solar cells. *Journal of Applied Physics* 1995; **77**: 3491–3504.
- Granek F and Zdanowicz T. Advanced system for calibration and characterization of solar cells. *OPTO-Electronics Review* 2004; **12**(1): 57–67.
- Pysch D, Mette A and Glunz SW. A review and comparison of different methods to determine the series resistance of solar cells. *Solar Energy Materials and Solar Cells*, 2007; **91**: 1698–1706.
- Rajkanan K and Shewchun J. A better approach to the evaluation of the series resistance of solar cells. *Solid-State Electronics*, 1979; **22**: 193–197.
- Chen PJ, Pao SC, Neugroschel A and Lindholm FA. Experimental determination of series resistance of p–n junction diodes and solar cells. *Electron Devices. IEEE Transactions on*. 1978; **25**: 386–388.
- Chaffin RJ and Osbourn GC. Measurement of concentrator solar cell series resistance by flash testing. *Applied Physics Letters* 1980; **37**: 637–639.
- Boucher J, Lescure M and Vialas J. Determination of series resistance of a solar cell by dynamic methods. *Photovoltaic Solar Energy Conference, Luxembourg*, 1977; 1044–1055.
- IEC 60891. Procedures for temperature and irradiance corrections to measured I–V characteristics of crystalline silicon photovoltaic devices. International Electrotechnical Commission 1987.
- Armin GA, Jan S and Rolf B. On the data analysis of light biased photoconductance decay measurements. *Journal of Applied Physics* 1996; **79**: 1491–1496.
- Schmidt J. Measurement of differential and actual recombination parameters on crystalline silicon wafers [solar cells]. *Electron devices. IEEE Transactions on*. 1999; **46**: 2018–2025.
- Sinton RA and Cuevas A. A quasi-steady-state open-circuit voltage method for solar cell characterization. *16th European Photovoltaic Solar Energy Conference, Glasgow*, 2000; 1152–1155.
- Burgers AR, Eikelboom JA, Schonecker A and Sinke WC. Improved treatment of the strongly varying slope in fitting solar cell I–V curves. *Photovoltaic Specialists Conference, Conference Record of the Twenty Fifth IEEE, Washington*, 1996; 569–572.
- McIntosh KR. Lumps, humps and bumps. Three detrimental effects in the current-voltage curve of silicon

- solar cells. Doctor of Philosophy Thesis, University of New South Wales, 2001.
25. Aberle AG, Glunz S and Warta W. Impact of illumination level and oxide parameters on Shockley-Read-Hall recombination at the Si-SiO<sub>2</sub> interface. *Journal of Applied Physics* 1992; **71**: 4422–4431.
26. Cousins PJ and Cotter JE. The influence of diffusion-induced dislocations on high efficiency silicon solar cells. *Electron devices. IEEE Transactions on*. 2006; **53**: 457–464.
27. Macdonald D. Impact of nickel contamination on carrier recombination in n- and p-type crystalline silicon wafers. *Applied Physics A: Materials Science & Processing*. 2005; **81**: 1619–1625.